Cancer Chemother Pharmacol (2011) 67:293–304
DOI 10.1007/s00280-010-1319-8

ORIGINAL ARTICLE

A novel bis-indole destabilizes microtubules and displays potent in vitro and in vivo antitumor activity in prostate cancer

Sunjoo Ahn · Dong Jin Hwang · Christina M. Barrett · Jun Yang · Charles B. Duke III · Duane D. Miller · James T. Dalton

Received: 11 December 2009 / Accepted: 28 March 2010 / Published online: 11 April 2010
© Springer-Verlag 2010

Abstract
Purpose Microtubules are one of the most useful subcellular targets in chemotherapy. We identified a novel indole, (3-(1H-indol-2-yl)phenyl)(1H-indol-2-yl)methanone (**15**), that inhibits tubulin action and exhibits potent antitumor activity in various preclinical models.
Methods In vitro cancer cell growth inhibition was measured by SRB or MTT assay in human cancer cell lines. Apoptosis induced by **15** was examined in LNCaP and PC-3 cells. Effects of **15** on cell cycle distribution and tubulin were investigated via in vitro models. In vivo toxicity and xenograft efficacy studies were conducted in mice.
Results Indole **15** inhibited the in vitro growth of a number of human cancer cell lines, including drug-resistant cell lines that over-express P-glycoprotein, multidrug resistance-associated proteins, and breast cancer resistance protein with IC_{50} values in the range of 34–162 nM. Nanomolar concentrations of the compound caused down-regulation of bcl-2, induced PARP cleavage, and induced apoptosis in both LNCaP and PC-3 prostate cancer cells, as confirmed by anti-histone ELISA and DNA laddering. In vitro studies revealed that the compound inhibited polymerization of purified tubulin and induced a strong and concentration-dependent G_2M arrest in PC-3 cells. In vivo studies in immunodeficient mice bearing PC-3 tumor xenografts showed that the compound effectively inhibited tumor growth.
Conclusions The potent in vitro and in vivo antitumor activities of this novel indole suggest that drugs with this novel chemical scaffold might be developed for treatment of drug-resistant prostate cancer.

Keywords Indole · Tubulin · Prostate cancer · MDR

Abbreviations

MRP	Multidrug resistance-associated proteins
BCRP	Breast cancer resistance protein
MDR	Multidrug resistance
ABC	ATP-binding cassette
SRB	Sulforhodamine B
MTT	3-(4,5-Dimethylthiazol-2-yl)-2,5-diphenyltetrazolium bromide
FACS	Fluorescence-activated cell sorting
MTD	Maximally tolerated dose
T/C	Treated over control tumor volume ratio × 100%

Introduction

Tubulin inhibitors are a major group of antitumor agents. Microtubules are critically important for the formation of

Electronic supplementary material The online version of this article (doi:10.1007/s00280-010-1319-8) contains supplementary material, which is available to authorized users.

S. Ahn · J. Yang · J. T. Dalton
Division of Pharmaceutics, College of Pharmacy, The Ohio State University, Columbus, OH, USA

S. Ahn · D. J. Hwang · C. M. Barrett · D. D. Miller · J. T. Dalton (✉)
Preclinical Research and Development, GTx, Inc., 3 North Dunlap Street, Memphis, TN 38163, USA
e-mail: jdalton@gtxinc.com

C. B. Duke III · D. D. Miller
Department of Pharmaceutical Sciences, College of Pharmacy, University of Tennessee, Memphis, TN, USA

the mitotic spindle, which dictates the proper segregation of chromosomes during mitosis. It is generally accepted that the anti-proliferative properties of microtubule-interacting drugs arise largely from their interactions with tubulin resulting in disruption of microtubule dynamics [1]. These drugs are commonly classified into two major categories: the microtubule-destabilizing agents (i.e., the vinca alkaloids and colchicines) and the microtubule-stabilizing drugs (i.e., taxanes). The vinca alkaloids, targeting the vinblastine-binding site, are effectively used to treat a wide variety of human cancers including hematological malignancies, breast, non-small-cell lung, and testicular carcinoma. Colchicine, which binds at a different site on β-tubulin, is used clinically for gout, but not cancer. Taxanes are also widely used in ovarian, breast, and non-small-cell lung carcinomas and bind to distinct binding sites on tubulin other than the vinblastine and colchicine sites. Docetaxel, a taxane analog, was the first chemotherapeutic agent specifically approved for the treatment of advanced prostate cancer by the US Food and Drug Administration in 2004 [2]. The clinical success of targeting tubulin for anticancer drugs has led to the search for new agents that inhibit tubulin activity with an improved safety profile. Tubulin inhibitors in human chemotherapy have severe limitations such as high peripheral neurotoxicity, low bioavailability, poor solubility, complicated synthesis procedures, and drug resistance mediated by multidrug resistance (MDR) transporters and tubulin mutation [1, 3–5].

High levels of intrinsic MDR transporters and their over-expression induced by long-term exposure to chemotherapy have been recently suggested as one of the reasons for the low chemotherapeutic responses in primary cell cultures from prostate cancer patients [6]. P-glycoprotein is a member of large family of ATP-binding cassette (ABC) including multidrug resistance-associated protein (MRP) and breast cancer resistance protein (BCRP) that are responsible for drug efflux and MDR. Cancer cells expressing P-glycoprotein are resistant to a number of structurally unrelated agents including vinca alkaloids, taxanes, colchicines, epipodophyhllotoxins, and anthracyclines with overlapping but not identical substrate specificity [7]. To date, no clinical solutions exist to overcome MDR caused by P-glycoprotein expression, but many research groups are actively pursuing different therapies to diminish this dilemma. In vivo and in vitro studies using some anticancer drugs that are not substrates of P-glycoprotein and therefore are not susceptible to being extruded from tumor cells have been reported. Epothilones, a new class of microtubule stabilizers, and 2-aroylindoles, orally active small molecule tubulin inhibitors, are recent examples of such agents [8–13]. Ixabepilone, an epothilone analog, is currently in phase II clinical trials for hormone-resistant metastatic prostate cancer, but thus far no results have been reported as to the success of the trial in http://clinicaltrials.gov.

The structural complexity of the vinca alkaloids, taxanes, and natural and marine-derived products [4] that inhibit tubulin presents a formidable challenge to organic medicinal chemists to develop feasible and high yield syntheses. Therefore, this limits the use of conventional, broad-scale screening approaches to characterize structure–activity relationships, identify active compounds, and proceed to preclinical and clinical evaluation.

During our studies to identify new pharmacophores for prostate cancer, we identified a novel class of indoles that act as potent anticancer agents. Indoles that inhibit tubulin action but circumvent MDR represent a novel chemical approach to this dilemma. We examined the sensitivity of a variety of human cancer cell lines to our lead, (3-(1H-indol-2-yl)phenyl)(1H-indol-2-yl)methanone (hereafter referred to as **15**; Table 1), and explored underlying mechanisms to explain the ability of **15** to induce apoptosis. We further compared the anticancer activity and toxicity of **15** to vinblastine and docetaxel in a human prostate cancer PC-3 xenograft model and provide compelling evidence that **15** is the first member of a new class of tubulin inhibitors that circumvent ABC transporter-mediated drug resistance with an improved safety profile compared to existing agents and other tubulin inhibitors in development.

Materials and methods

Chemistry

All investigational compounds were made using the synthetic scheme shown in Fig. 1, with compounds **7** and **10** serving as common intermediates. Two Suzuki coupling pathways were used for the synthesis of the indole benzaldehyde **7**. In Path A, **7** was prepared via the lithiation of commercially available 1-(phenylsulfonyl)-1H indole, **2** by lithium diisopropylamide (LDA) followed by bromination with cyanogen bromide (BrCN) to produce **5** for coupling with 3-formylphenylboric acid. In Path B, commercially available indole boric acid, **6** and 3-iodophenylaldehyde were coupled to yield **7**. **10** was synthesized by coupling **7** with activated **2** using LDA. **11** was made using triethylsilane and trifluoroacetic acid at room temperature to reduce the methanol linkage of **10**, while **14** was made from **10** via the oxidation of the methanol linkage with pyridinium dichromate in DMF. **12**, **13**, and **15** were then synthesized by de-protection of **10**, **11** and **14**, respectively,

Table 1 IC_{50} values of different cancer cell lines treated with indoles by the SRB assay

Compound ID, structure	IC_{50} (μM)						
	LNCaP	PC-3	DU-145	PPC-1	TSU-Pr1	MCF-7	HT-29
Vinblastine	0.003 ± 0.001	0.001 ± 0.0003	0.003 ± 0.001	0.001 ± 0.0004	0.002 ± 0.0001	0.001 ± 0.0004	0.002 ± 0.0002
Docetaxel	0.005 ± 0.001	0.006 ± 0.0004	0.005 ± 0.001	0.003 ± 0.001	0.003 ± 0.001	0.004 ± 0.001	0.004 ± 0.0002
1 [34] 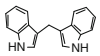	5.8 ± 0.5	39.4 ± 1.7	39.7 ± 2.6	31.8 ± 1.1	45.7 ± 1.1	32.2 ± 2.7	>50
3 	>100	>100	>100	>100	>100	ND	ND
4[a] 	18.3 ± 1.4	59.9 ± 1.8	55.1 ± 2.5	41.1 ± 1.8	39.3 ± 1.6	ND	ND
5[a] 	29.6 ± 2.2	69.3 ± 2.1	63.9 ± 1.9	52.1 ± 1.1	44.9 ± 2.0	ND	ND
6[a] 	23.1 ± 4.0	73.9 ± 7.1	72.0 ± 3.4	80.8 ± 1.2	48.2 ± 3.4	ND	ND
7[a] 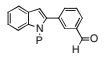	17.7 ± 1.2	23.2 ± 1.4	19.7 ± 1.3	13.9 ± 0.2	11.5 ± 0.1	ND	ND
8 	23.8 ± 3.0	65.1 ± 5.3	ND	ND	ND	ND	ND
9 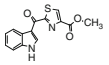	58.5 ± 14.3	90.4 ± 27.5	ND	ND	ND	ND	ND
10[a] 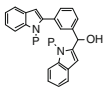	>100	>100	>100	20–40	>100	ND	ND
11[a] 	>100	>100	>100	>100	>100	ND	ND
12 	>50	>50	ND	>50	20–50	10.4 ± 0.9	0.72 ± 0.02
13 	5.6 ± 1.1	13.5 ± 0.4	ND	ND	ND	ND	ND
14[a] 	>100	>100	>100	>100	>100	>100	ND
15 	0.044 ± 0.002	0.081 ± 0.010	0.138 ± 0.013	0.067 ± 0.001	0.034 ± 0.018	0.162 ± 0.010	0.062 ± 0.008

Each value represents the mean ± SD of three independent experiments

ND not determined

[a] In the structure: P = $-SO_2Ph$

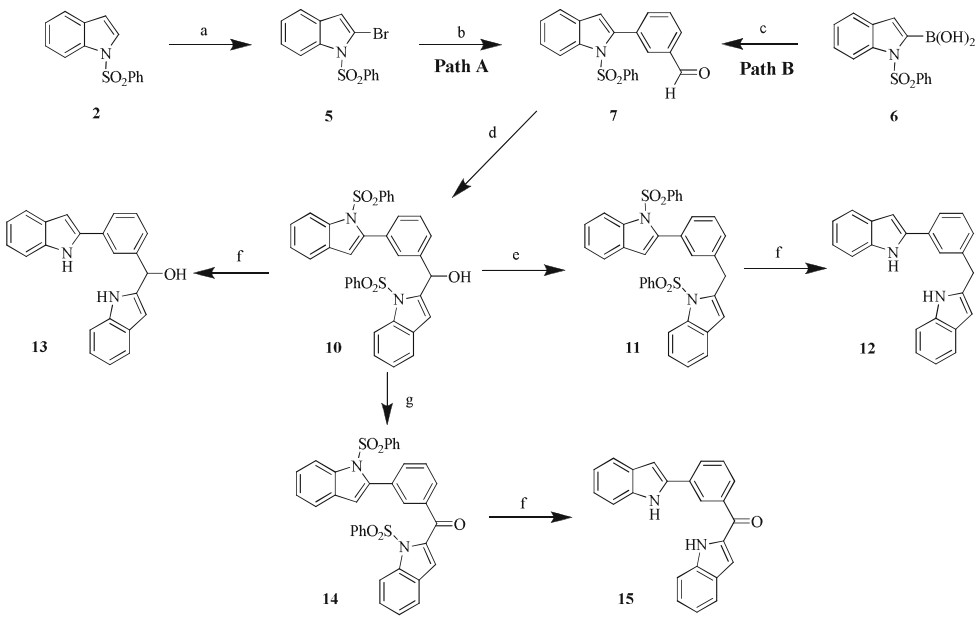

Fig. 1 Synthesis scheme. Reagents and conditions: *a i.* LDA, THF, −78°C; *ii.* BrCN; *b* Path A; 3-formylphenylboronic acid, Na_2CO_3, $Pd(PPh_3)_4$, DME; *c* Path B; 3-iodobenzaldehyde, Na_2CO_3, $Pd(PPh_3)_4$, DME; *d* LDA, compound **1**, THF, −78°C; *e* Et_3SiH, CF_3CO_2H, CH_2Cl_2, room temperature; *f aq.* NaOH, EtOH, reflux; *g* pyridinium dichromate, room temperature

with reflux under basic conditions. The yields of all products were excellent (83–95%). Structures and purity were determined by NMR (^1H and ^{13}C), mass spectrometry and elemental analysis.

Chemicals and animals

Monoclonal antibodies and horseradish peroxidase-conjugated secondary antibodies were purchased from Santa Cruz Biotechnology, Inc. (Santa Cruz, CA). Bovine brain tubulin protein was purchased from Cytoskeleton, Inc (Denver, CO). [^{3}H]vinblastine and [^{3}H]podophyllotoxin were purchased from Moravek, Inc (Brea, CA). Sephadex G25 column and Cell Death Detection ELISA (anti-histone ELISA) were purchased from Roche Applied Science (Indianapolis, IN). All other chemicals were purchased from Sigma (St. Louis, MO).

Four- to 5-week-old male ICR mice and male nu/nu nude mice were purchased from Harlan Biosciences (Indianapolis, IN). All animal protocols were approved by the Animal Care and Use Committee at The Ohio State University or the University of Tennessee.

Cell culture

All human cancer cell lines except K562/DOX, HEK293-pcDNA3.1, HEK293-MRP1, HEK293-MRP2, HEK293-pcDNA3-10 and HEK293-482R2 were obtained from American Type Culture Collection (Manassas, VA). K562/DOX, HEK293-pcDNA3-10 and HEK293-482R2 were kindly provided by Dr. Duxin Sun (College of Pharmacy, The Ohio State University). The plasmids for MRP1 and MRP2 were kindly provided by Dr. Susan P. C. Cole (Department of Pharmacology & Toxicology, Queen's University) [14]. K562/DOX was obtained by in vitro selection of K562 in progressively increasing doses of doxorubicin [15, 16]. HEK293-MRP1 and HEK293-MRP2 were transfected with the plasmid encoding the full-length MRP1 and MRP2 genes, respectively, according to the calcium phosphate transfection method [17]. HEK293-pcDNA3.1 was transfected with empty pcDNA 3.1(−) vector. HEK293-MRP1, HEK293-MRP2, and HEK293-pcDNA3.1 cells were selected with 200 μg/mL G418 for 4 weeks after transfection. HEK293-pcDNA3-10 and HEK293-482R2 were HEK293 cells transfected with empty pcDNA3 vector and pcDNA3 vector containing full-length BCRP, respectively [18]. Cells were maintained in RPMI-1640 medium containing 2 mM L-glutamine supplemented with 10% fetal bovine serum. All cells were grown at 37°C in a humidified atmosphere containing 5% carbon dioxide. RPMI-1640 media, trypsin–EDTA and L-glutamine were purchased from Mediatech (Herndon, VA). FBS was purchased from Invitrogen (Carlsbad, CA).

Growth inhibition assay

The cytotoxic or anti-proliferative activity of test compounds was investigated in cancer cell lines using the sulforhodamine B (SRB) assay. The (3-(4,5-dimethylthiazol-2-yl)-2,5-diphenyltetrazolium bromide) (MTT) assay was also used for the leukemia cell lines. Cultured cells were plated into 96-well plates and incubated with medium containing different concentrations of the test compounds for 4 days. Cells were stained with SRB or MTT solution. The optical density was determined at 540 nm on a microplate reader (Dynex Technologies, Chantilly, VA).

The concentration that inhibited cell growth by 50% relative to the untreated control (IC_{50}) was determined by nonlinear least squares regression using WinNonlin software (Pharsight Corporation, Cary, NC). WinNonlin was provided by a Pharsight Academic License to The Ohio State University.

Determination of DNA fragmentation by ELISA

Apoptosis was measured by quantitation of cytoplasmic histone-associated DNA fragments using the cell death detection ELISA kit. LNCaP and PC-3 cells were seeded in six-well plates and exposed to **15** for 24 h at final concentrations of 100 and 200 nM (approximating the IC_{90} values in these cell lines), respectively. The quantitation of DNA fragments was performed according to the manufacturer's instructions.

DNA gel electrophoresis

Cells were treated with different concentrations of drugs. The cell pellet was treated with lysis buffer (50 mM Tris–HCl, pH 7.5, 20 mM EDTA, 1% NP-40) for 20 min at 4°C. After centrifugation, the supernatant was treated with RNase A (5 μg/μL) for 2 h at 56°C and proteinase K (2.5 μg/μL) for 6 h at 37°C. The DNA was precipitated with 100% ethanol (20°C). The pellet was then dissolved in TE buffer and loaded on a 1.2% agarose gel containing ethidium bromide. The apoptotic DNA was visualized by placing the gel on a UV transilluminator.

Cell cycle analysis

Treated cells were washed with PBS and fixed with 70% ice-cold ethanol overnight. Fixed cells were then stained with propidium iodide (20 μg/mL) in the presence of RNase A (300 μg/mL) at 37°C for 30 min. Cell cycle distribution was analyzed by fluorescence-activated cell sorting (FACS) analysis core services at The Ohio State University, Columbus, OH.

Western blot analysis

Treated cells were lysed in cold lysis buffer [20 mM Tris–HCl, pH 7.5, 150 mM NaCl, 1 mM Na_2–EDTA, 1% Triton-X 100, and freshly added Na_3VO_4 (2 mM), NaF (20 mM) and complete protease inhibitor cocktail]. For each sample, an aliquot (20–40 μg) of total protein was loaded and run on a SDS-PAGE gel. Protein was transferred to nitrocellulose membranes (Bio-Rad Laboratories, Hercules, CA), blocked with 5% non-fat milk, incubated with primary antibody overnight at 4°C, and then incubated with secondary antibody at room temperature for 1 h. The ECL™ (GE Healthcare Bio-Sciences Corp., Piscataway, NJ) was used for detection.

In vitro tubulin depolymerization assay

BK004 kits (Cytoskeleton, Denver, CO) were used to study tubulin depolymerization. The reaction contained 50 μL of 4 mg/mL tubulin in PEM buffer (80 mM PIPES, pH 7.0, 0.5 mM EGTA, 2 mM $MgCl_2$, 1 mM GTP, 10% glycerol). The procedure was done according to the manufacturer's protocol. Tubulin polymerization was monitored in a UV spectrophotometer for 40 min at 340 nm at 37°C.

Indirect immunofluorescence microscopy

PC-3 cells were plated on poly-D-lysine-coated glass coverslips in six-well plates (2.5×10^4 cells/well) the day before treatment. After cells were incubated with cytotoxic agents at 37°C for 6 h, cells were fixed on coverslips with 4% formaldehyde in PBS for 10 min and permeabilized by 2% Triton-X in PBS for 5 min. They were blocked with 3% bovine serum albumin in TBST for 30 min and incubated with anti-α-tubulin-FITC antibody (Sigma, St. Louis, MO) used at 1:100 dilution at 4°C overnight. They were mounted on slides and observed by a Zeiss Axioplan 2 fluorescent microscope (Carl Zeiss, Thornwood, NY). Images were acquired with a Zeiss Axiocam HRc, using Zeiss AxioVision.

In vitro binding assay by spin column

A spin column binding assay was used to determine whether **15** competes for either the vinblastine- or colchicine-binding sites [19]. Tubulin (0.1 mg/mL) was incubated either with 3 μM vinblastine containing [^{3}H]vinblastine (4×10^4 dpm/nmol) in the presence of different concentrations of vincristine or **15** in PEM buffer or with 3 μM podophyllotoxin containing [^{3}H]podophyllotoxin (4×10^4 dpm/nmol) in the presence of different concentrations of colchicine or **15** in PEM buffer in a total volume of 140 μL at 37°C for 1 h. Samples (120 μL) were then loaded onto size-exclusion Sephadex G25 columns that were pre-washed with 3 mL of PEM buffer. The columns were then placed into empty tubes and centrifuged at 200*g* for 1 min and radioactivity in the flow-through was analyzed by scintillation counting.

In vivo antitumor efficacy study

PC-3 cells (2.5×10^6 cells/site) were injected subcutaneously into the flanks of male nu/nu mice. Tumor size was

measured using calipers every 3 days and calculated as $V = \pi/6 \times (\text{length}) \times (\text{width})^2$ [20]. When tumors reached a volume of approximately 150 mm^3, drug treatment was initiated. The control group was treated with vehicle (10% DMSO in PEG300) only. During the treatment, tumor size and animal body weight were measured twice per week. Relative tumor growths (%) were calculated considering the mean tumor volumes at day 0 as 100%.

Statistical analysis

The results (mean values ± SD) were subjected to statistical analysis by single-factor ANOVA. The level of significance was set at $P < 0.05$.

Results

The effect of indoles on cell proliferation

Structural variations were introduced in the methylene spacer (i.e. CH_2, CH–OH or C=O) between the phenyl group and indole-ring for analysis of structure–activity relationships. **15**, with a methanone linkage, demonstrated the most potent growth inhibitory effects in several human cancer cell lines of differing tissue origin, including prostate cancer cell lines DU-145, LNCaP, PC-3, and PPC-1, bladder cancer TSU-Pr1 cells, breast adenocarcinoma MCF7 cells, and the colorectal carcinoma HT29 cell line (Table 1). IC_{50} values for **15** ranged from 33.8 to 162 nM. Reduction of the methanone linkage to an alcohol **13** significantly reduced activity, with IC_{50} values over 100-fold higher for **13** in LNCaP and PC-3 cells as compared to **15**. Complete reduction to a methylene linker **12** almost completely abolished activity. Protected compounds (**10**, **11**, and **14**) were devoid of activity, while partial intermediates (**3** through **9**) and a bis-indole with a simple methylene linker **1** also demonstrated substantially reduced activity in these cancer cell lines. Vinblastine and docetaxel confirmed the assay validity by exhibiting high potency in cancer cell lines with IC_{50} values ranging from 1.05 to 6.3 nM.

The effect of **15** on growth of cells that over-express P-glycoprotein, MRPs, and BCRP

We next determined whether cells that over-express P-glycoprotein, MRP1, MRP2, and BCRP were resistant to **15**. To examine the P-glycoprotein-induced drug resistance, the parental K562 leukemia cell line and its doxorubicin-resistant sub-line (K562/DOX) that over-expresses P-glycoprotein were co-incubated with different concentrations of **15**, doxorubicin, docetaxel, paclitaxel, and vinblastine. It is well established that doxorubicin, docetaxel, paclitaxel, and vinblastine are substrates for P-glycoprotein [21]. The IC_{50} values for doxorubicin, vinblastine, docetaxel, and paclitaxel were increased 32-, 191-, 203-, and 121-fold, respectively, in the K562/DOX cell line as compared to parental K562 cells, while **15** demonstrated equal potent anticancer activity in the two cell lines (Table 2).

Studies were performed using MDR-expressing HEK293-MRP1 and HEK293-MRP2 cells treated with **15** to determine if **15** is a substrate for MRP1 and MRP2. Vinblastine, doxorubicin, SN-38, and docetaxel were substantially less effective in HEK293-MRP1 and HEK293-MRP2 (Table 2). IC_{50} values for vinblastine, doxorubicin, SN-38, and docetaxel were 4.9-, 3.7-, 2.1- and 7.2-fold greater in cells with high MRP1 expression and 3.7-, 2.2-, 1.5-, and 7.6-fold greater in cells over-expressing MRP2 than in HEK293-pcDNA3.1 empty vector cells. **15**, however, demonstrated similar IC_{50} values in HEK293-pcDNA3.1 and HEK293-MRP1 and HEK293-MRP2 cells.

For the BCRP transporter, HEK293 cells transfected with pcDNA3 empty vector and HEK293-482R2 transfected with the vector including BCRP gene were used. Upon treatment with SN-38 and vinblastine, significant differences between the IC_{50} values in HEK293-pcDNA3-10 and HEK293-482R2 cell line were seen (Table 2). IC_{50} values for SN-38 and vinblastine were 33- and 4-fold greater, respectively, in cells with high BCRP expression as compared to nonexpressing cells. **15**, however, retained similar potency in HEK293-482R2 cells, as well as K562/DOX, HEK293-MRP1, and HEK293-MRP2 cell lines as compared to the control cell lines. These data indicate that **15** is not a substrate for P-glycoprotein, MRP1, MRP2, and BCRP, while other chemotherapeutic agents that target tubulin (vinblastine, docetaxel, and paclitaxel) or other cellular mechanisms (SN-38 and doxorubicin) are substrates for these ABC transporters.

Apoptotic effect induced by **15**

In the apoptosis study using the cell death detection ELISA kit, **15** increased the enrichment factor (absorbance in treated cells/absorbance in control cells) 4.5- and 4-fold in LNCaP and PC-3 cells, respectively ($P < 0.05$; Fig. 2a). The extent of apoptosis was greater in LNCaP as compared to PC-3 cells, which is consistent with the lower IC_{50} value of **15** in LNCaP (44 nM) versus PC-3 cells (81 nM). DNA laddering results also suggested that **15** induced significant apoptosis in both cell lines (Fig. 2b). After a 48-h incubation of **15** (100 nM) in LNCaP cells, a similar extent of DNA laddering was observed as compared to that induced by 50 nM paclitaxel (Fig. 2b). As a whole, these studies

Table 2 Effect of **15** and other agents on the growth of cells expressing ABC MDR transporters

Resistance phenotype and cell line	IC_{50} (nM)					
	15	Doxorubicin	Vinblastine	SN-38	Docetaxel	Paclitaxel
P-glycoprotein						
K562	63.6 ± 2	27.1 ± 6	1.4 ± 0.4	ND	2.7 ± 1.0	12.2 ± 0.2
K562/DOX	78.2 ± 3 (1.2)	859 ± 27 (31.7)	268.1 ± 48 (191)	ND	548.5 ± 76 (203)	1480 ± 479 (121)
MRP						
HEK293-pcDNA3.1	60.2 ± 7	80.6 ± 3	5.0 ± 1	8.4 ± 1	4.4 ± 2	ND
HEK293-MRP1	89.9 ± 13 (1.5)	298.1 ± 16 (3.7)	24.3 ± 2 (4.9)	17.7 ± 1 (2.1)	31.3 ± 5 (7.2)	ND
HEK293-MRP2	90.4 ± 2 (1.5)	177.6 ± 11 (2.2)	18.1 ± 4 (3.7)	12.4 ± 1 (1.5)	33.1 ± 4 (7.6)	ND
BCRP						
HEK293-pcDNA3-10	91.6 ± 10	ND	4.04 ± 0.8	2.9 ± 0.3	ND	ND
HEK293-482R2	105 ± 4 (1.15)	ND	15.7 ± 2 (3.89)	94.3 ± 20 (32.5)	ND	ND

P-glycoprotein, MRP1, MRP2, BCRP were over-expressed in K562/DOX, HEK293-MRP1, HEK293-MRP2 and HEK293-482R2. The resistance factor (in parentheses) was calculated as the ratio of IC_{50} values for the resistant cell sub-line to that of the parental cell line. All experiments were performed at least in three replicates

ND not determined

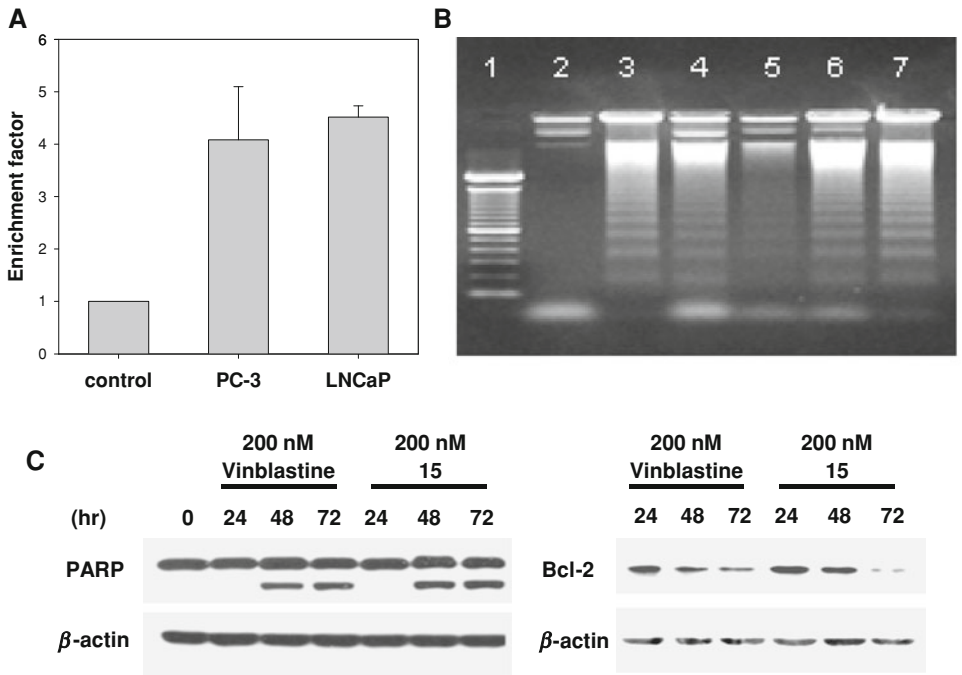

Fig. 2 Apoptosis induced by **15** treatment. **a** **15** induces histone and DNA fragmentation in LNCaP and PC-3 cells. Cells were incubated with **15** at a concentration of IC_{90} to each cell line for 24 h. The extent of apoptosis (i.e., the enrichment factor) was determined using a commercially available anti-histone ELISA. **b** DNA ladder from LNCaP cells treated with different concentrations of drugs for different time was obtained by 1.2% agarose gel electrophoresis. *1* 100 bp DNA marker, *2* vehicle-treated, *3* 50 nM paclitaxel (72 h), *4*, *5* 100 nM **15** (48, 72 h), *6*, *7* 500 nM **15** (48, 72 h). **c** PARP cleavage and decreased expression of Bcl-2 were observed in PC-3 cells treated with 200 nM of vinblastine and **15** for 24, 48 and 72 h by Western blot analysis

provide persuasive evidence that **15** potently induces apoptosis in prostate cancer cell lines, with potency similar to but slightly less than paclitaxel.

To further elucidate the apoptotic mechanism of **15**, we examined its effects on PARP cleavage, a marker of apoptotic cell death, and the expression of the anti-apoptotic protein bcl-2 in PC-3 cells after 24-, 48-, and 72-h treatments (Fig. 2c). Lysates of PC-3 showed no cleavage of PARP and a high expression of bcl-2 before drug treatment. PARP cleavage was observed after 48-h exposure with **15** (200 nM; approximate IC_{90} value in PC-3 cell growth inhibition study). Bcl-2 expression decreased in

a time-dependent manner after treatment with **15** (200 nM), suggesting that **15**-induced apoptosis is at least partially mediated by down-regulation of bcl-2.

Effect of **15** in cell cycle distribution

As an initial step to understand the mechanism of action of **15**, we determined the effect of **15** on the cell cycle. The percentage of PC-3 cells in G_2M phase increased (Fig. 3a) from 13% (control) to 24, 46, and 73% at **15** concentrations of 100, 300, and 500 nM, respectively, indicating that PC-3 cells were significantly arrested in the G_2M phase in a concentration-dependent manner, a pattern that is commonly observed with taxanes and vinca alkaloids. When the percentages of cells in G_2M phase were plotted against different concentrations of the compounds (0.1 nM–1 μM), vinblastine, docetaxel, and **15** arrested the cell cycle with EC_{50} values of 7, 14, and 282 nM, respectively (Fig. 3a). The effect of these drug arresting cells in the G_2M phase is closely related to their IC_{50} values of cytotoxicity in PC-3 cells (1, 6, and 81 nM, respectively; Table 1), suggesting that this is a direct link to their mechanism of action.

The effect of **15** on microtubule polymerization

Vinblastine and **15** were compared for their ability to inhibit tubulin polymerization at different concentrations of the compounds. Microtubule polymerization was measured by absorbance over time since assembled microtubules cause turbidity in the assay solution (Fig. 3b). These data indicate that **15** mimics the effects of vinca alkaloids on tubulin polymerization to reduce polymerization and destabilize microtubule formation as is evident by the decrease in absorbance with increasing concentration. **15** suppressed tubulin polymerization in a concentration-dependent manner with an IC_{50} of 554 nM, whereas the IC_{50} of vinblastine was 283 nM (Fig. 3b). In order to visualize the microtubule changes in the cells, immunofluorescence microscopy was used. Vinblastine inhibited microtubule polymerization with the appearance of short microtubule fragmentations in the cytoplasm. In contrast, treatment with docetaxel resulted in stabilization of microtubule with an increase in the density of microtubules. Treatment with **15** induced similar changes to microtubules as compared to vinblastine (Fig. 3c).

In vitro competition of binding of vinblastine or podophyllotoxin to tubulin by **15**

Antimitotic agents are known to bind at different binding sites in the tubulin protein. Since microtubule polymerization inhibitors usually bind to the vinblastine- or colchicine-binding sites, we assessed the binding of **15** to tubulin with [^{3}H]vinblastine and [^{3}H]podophyllotoxin (binds to the colchicine site) in a competition binding assay using vincristine and colchicine as positive control inhibitors. When depolymerized tubulin was incubated with radiolabeled vinblastine in the presence of different concentrations of the unlabeled vincristine, a known competitor of vinblastine binding to tubulin, the amount of protein-bound [^{3}H]vinblastine found in the flow-through was strongly reduced (Fig. 3d). Thus, vincristine competes for the binding of vinblastine to tubulin. However, when different concentrations of **15** instead of vincristine were used, no effect on binding of [^{3}H]vinblastine to tubulin was observed (Fig. 3d). When tubulin was incubated with [^{3}H]podophyllotoxin in the presence of different concentrations of unlabeled colchicine, the amount of [^{3}H]podophyllotoxin in the flow through the column was reduced (Fig. 3d). Thus, podophyllotoxin competes for the binding of colchicine to tubulin. Increasing concentrations of **15** also decreased [^{3}H]podophyllotoxin binding to tubulin, indicating that **15** binds to the colchicine-binding site to induce disassembly of microtubules (Fig. 3d).

In vivo pharmacology of **15**

The acute toxicity (as measured by changes in morbidity in 24 h) of vinblastine and **15** was examined in ICR mice via IV injection to identify the maximally tolerated dose (MTD). The acute MTD of vinblastine was 25 mg/kg, whereas **15** did not induce any severe acute toxicity at doses up to 500 mg/kg. For sub-chronic toxicity, doses were administered via IP injection (5 days/week) in ICR mice. The positive control group was divided into groups of five and received vinblastine doses of 25, 5, 2.5, 1, and 0.5 mg/kg. For **15**, mice were divided into four groups that received 250, 125, 50, and 25 mg/kg. There was no significant difference in morbidity in 2.5, 1, and 0.5 mg/kg vinblastine or in any **15** treatment groups. These results suggest that **15** was well tolerated with up to 4-week treatment.

We further examined the effects of **15** (5 and 25 mg/kg, i.p., 2 days/week and 10 mg/kg, i.p., q2d) on in vivo tumor growth for 4 weeks in a PC-3 xenograft model. Vinblastine- (0.5 mg/kg) and docetaxel-treated (5 mg/kg) mice were included as a positive control. Tumor size in the vehicle control group increased seven- to eightfold over a period of 4 weeks. **15** (25 mg/kg) and vinblastine (0.5 mg/kg) twice weekly treatment resulted in 40 and 50% T/C (treated over control tumor volume ratio × 100%), respectively (Fig. 4a). Also with this dosing regimen, 5 mg/kg docetaxel inhibited tumor growth with 21% T/C, but induced a greater than 15% body weight loss after 2 weeks. In addition, the survival rate of docetaxel treated mice was

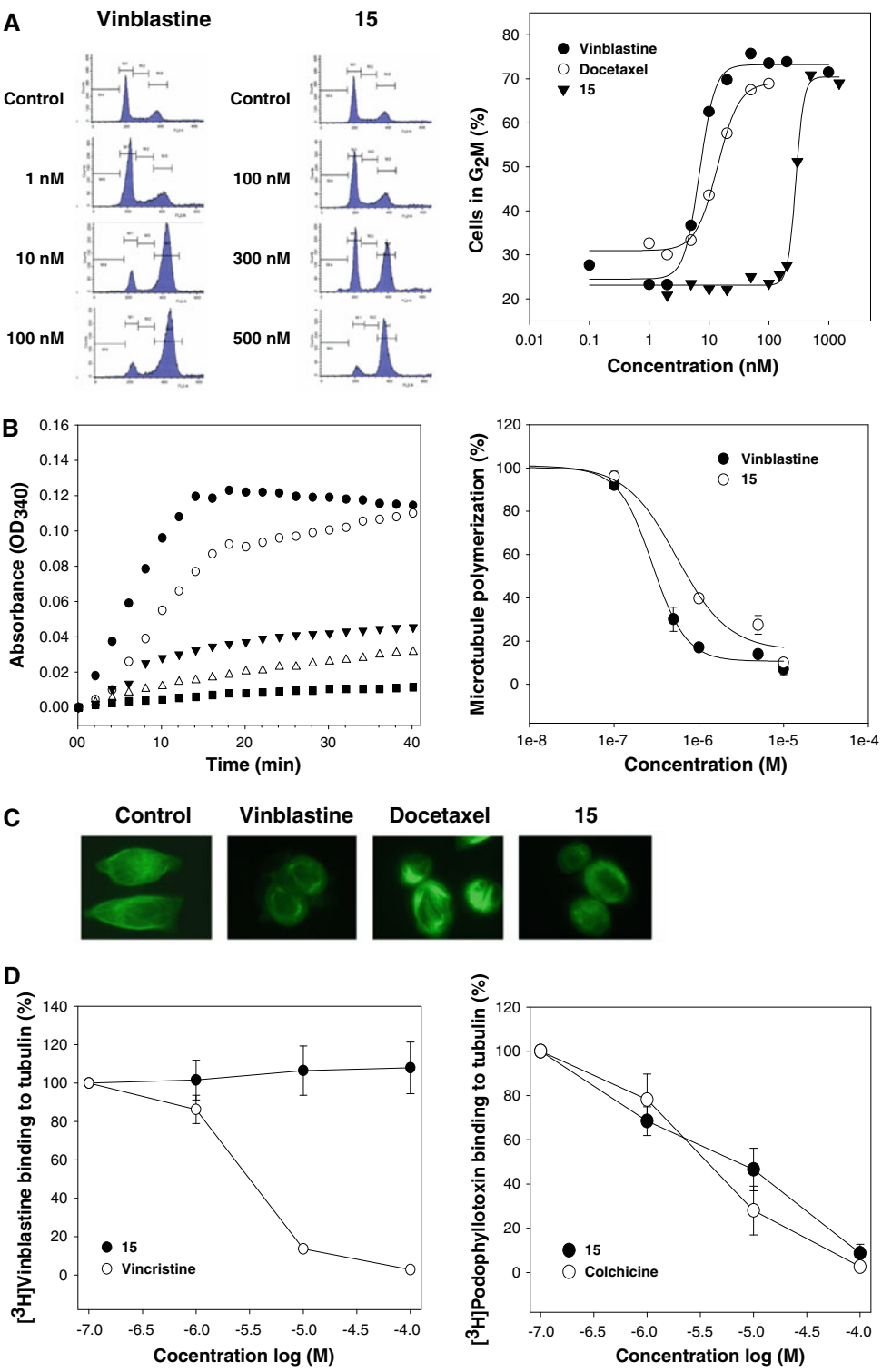

Fig. 3 Effect of **15** on cell cycle and tubulin. **a** PC-3 cells were treated with different concentrations (0–1.5 μM) of **15**, vinblastine, or docetaxel for 24 h, and DNA content of the cells was analyzed by FACS. The percentage of cells in G_2M phase of the cell division cycle was quantified. Selected FACS histograms (*left panel*) and dose response curves (*right panel*) were shown. **b** The microtubule polymerization was monitored by measuring the turbidity at 340 nm in the absence or presence of drugs (*right panel*). Representative experiment. Control (*filled circles*); **15**, 0.1 μM (*open circles*); **15**, 1 μM (*filled triangles*); **15**, 5 μM (*open triangles*); **15**, 10 μM (*filled squares*). Data shown are the mean of duplicate reaction. Dose-dependent curve was shown (*left panel*). **c** PC-3 cells were treated with 2 μM of antimitotic agents for 6 h. Fixed cells were reacted with anti-α-tubulin-FITC antibody and the cellular microtubules were observed by a Zeiss Axioplan 2 fluorescent microscope. **d** Competition of **15** for colchicine- or vinblastine-binding sites on tubulin was investigated in spin column assay. [^{3}H]vinblastine was incubated with tubulin in the presence of different concentrations of vincristine or **15** (*left panel*). [^{3}H]podophyllotoxin was incubated with tubulin in the presence of different concentrations of colchicine or **15** (*right panel*). Tubulin-bound [^{3}H]vinblastine and [^{3}H]podophyllotoxin were plotted against the concentrations of the competitors

70% after 3 weeks and less than 30% after 4 weeks, while **15**- and vinblastine-treated groups had 100% survival. A second xenograft study with q2d dosing schedule resulted in comparable efficacy of the 10 mg/kg **15** and 0.5 mg/kg vinblastine (Fig. 4b) with 42 and 38% T/C, respectively. Unfortunately, docetaxel (5 mg/kg) treatment following every other day dosing was too toxic. **15** was also well tolerated with no signs of toxicity with an increased dosing schedule. Loss of body weight after treatment was <15% of the initial body weight in all treatment groups receiving **15**

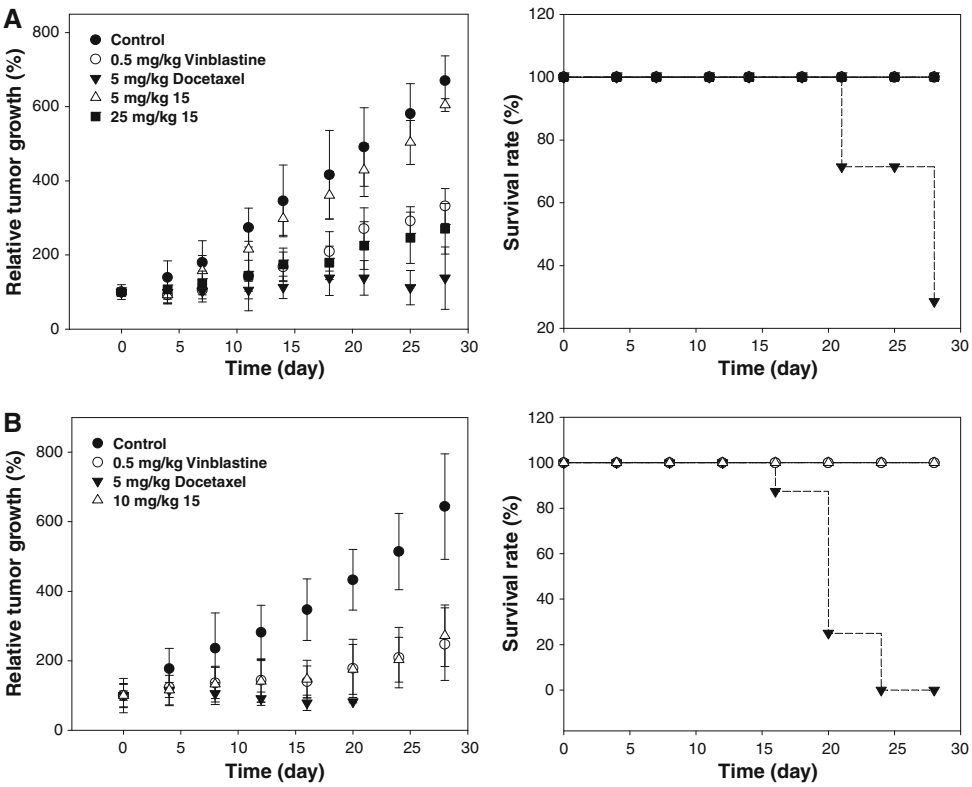

Fig. 4 Efficacy of **15**. **a** PC-3 xenografts were treated with vehicle control, vinblastine (0.5 mg/kg, i.p.; 2 days/week), docetaxel (5 mg/kg, i.p.; 2 days/week), and **15** (5 and 25 mg/kg, i.p.; 2 days/week). **b** PC-3 xenografts were treated with vehicle control, vinblastine (0.5 mg/kg i.p.; q2d), docetaxel (5 mg/kg, i.p.; q2d), and **15** (10 mg/kg, i.p.; q2d). The relative tumor growths (%) and body weights were plotted against time and are the mean ± SD from six to eight animals

(Fig. 4). Thus, **15** exerts potent antitumoral efficacy toward PC-3 solid tumor xenografts without any general toxicity.

Discussion

Indole derivatives have been a major interest in anticancer drug development for decades. Indole-3-carbinol and diindolymethane demonstrated apoptotic effects in human breast and prostate cancer cell lines in vitro [22, 23] and a great number of novel indole compounds have been investigated for antimitotic effects such as BpR0L075, D-24851, aroylindoles, tryprostatin A, and 2-acyl-1H-indole-4,7-diones [11, 19, 24–29]. During drug screening efforts, we identified a series of novel indoles that exhibit potent anticancer activities. These indoles were synthesized by Suzuki coupling pathways, oxidation, and de-protection and their activity evaluated against of a variety of human cancer cell lines. The most active compound, **15**, (3-(1H-indol-2-yl)phenyl)(1H-indol-2-yl)methanone was further studied to understand its basic mechanism of action and its potential use in vivo.

Apoptosis was induced by **15** at nanomolar concentrations in several prostate cancer cell lines including LNCaP, PPC-1, DU-145, and PC-3. Like other microtubule-destabilizing agents, **15** arrested cancer cells at the G_2M phase in a concentration-dependent manner by binding to the colchicine-binding site and preventing tubulin polymerization (Fig. 3).

P-glycoprotein is thought to be one of the major causes of failure of cancer therapy in the clinic. As such, the search has turned toward the identification of cytotoxic compounds that are not substrates for P-glycoprotein. **15** showed potent cytotoxic effects in cells expressing P-glycoprotein, as well as MRP1-, MRP2- and BCRP-positive cell lines (Table 2). These data suggest that **15** is a poor substrate of P-glycoprotein, MRP1, MRP2, and BCRP. The ability to retain activity in MDR over-expressing cell lines strongly supports the potential use of **15** in taxane- and vinca alkaloid-resistant cancer diseases.

We also investigated the involvement of **15** in an important cell survival pathway. It is known that microtubule damage leads to cancer cell apoptosis through inactivation of bcl-2, an important guardian of microtubule integrity [30]. In our Western blot study using PC-3 cells, vinblastine and **15** reduced the level of bcl-2 in a time-dependent manner (Fig. 2c). These agents, however, also induced cytotoxicity in DU-145 prostate carcinoma, which does not express bcl-2. The IC_{50} value of **15** in DU-145 cells was somewhat higher (138 nM) than the IC_{50} values in other prostate cancer cell lines (44–81 nM). These data suggest that microtubule-damaging agents induce apoptosis in connection with bcl-2 down-regulation, but that decreases in bcl-2 are not the only anticancer mechanism of antimitotic drugs. Docetaxel, a microtubule stabilizer, has

also been shown to be an effective inhibitor of tumor growth in DU-145 xenograft model, thus supporting a bcl-2 independent mechanism for tubulin inhibitors [31].

The in vivo toxicity study in ICR mice showed no severe toxicity of **15** at doses up to 250 mg/kg, the maximum dose tested. Since vinca alkaloids are widely used antimitotic agents in clinical chemotherapy, we used vinblastine as one of the positive controls during in vivo efficacy and toxicity studies. In addition, **15** was compared to docetaxel, a antimitotic taxane analog, which is the first approved chemotherapy for the treatment of advanced prostate cancer. A 25-fold lower dose of **15** (10 mg/kg) was shown to be as effective in the PC-3 xenograft model as 0.5 mg/kg vinblastine, a dose only fivefold lower than the sub-chronic MTD of vinblastine in the q2d regimen. Docetaxel showed severe body weight loss, as well as tumor growth inhibition. The body weight loss (>15%) in docetaxel group (5 mg/kg, i.p., 2 days/week) was observed with 33% T/C after 2-week treatment. Docetaxel was very efficacious (21% T/C) but less than 30% of the mice survived by the end of this study. **15** (10 mg/kg, i.p., q2d) induced tumor growth inhibition (42% T/C) with no signs of general toxicity. Ixabepilone (BMS-247550), the most widely clinically investigated epothilone, produced significant antitumor activities at doses between 6.6 and 15 mg/kg (q4d 3×, i.v.), but the MTD of ixabepilone was between 10 and 16 mg/kg (q4d 3×, i.v.) in several mice xenograft models [10, 32, 33]. Our data suggest that **15** may also provide a wider therapeutic window between efficacy and toxicity than available agents or ixabepilone, perhaps due to its utilization of the colchicine-binding site in tubulin. More definitive animal studies to examine the general safety and neurotoxicity of indole 15 are on-going in our laboratory.

Clinical use of indole alkaloids is currently restricted to vinblastine, vincristine and vinorelbine, all of which target the vinca alkaloid binding site in tubulin. Although a number of agents are undergoing early clinical trials, there are no therapies available for clinical use that bind the colchicine-binding site and avoid MDR. The relatively large structural complexity of vinca alkaloids and taxanes has remained a challenge for industry to develop a feasible synthesis. In this study, we show that a simple molecule, **15**, elicits high anticancer activity by targeting the colchicine-binding site in a broad spectrum of human cancer cells including ABC transporter positive cell lines. As a whole, our pilot in vivo anticancer activity and MDR insensitivity of **15** validates the development of structurally related antimitotic agents against prostate cancer and other paclitaxel, vinca alkaloid or MDR cancers.

Acknowledgments These studies were supported by grant #PC060380 from the Department of Defense Prostate Cancer Research Program of the US Army Medical Research and Materiel Command.

References

1. Dumontet C, Sikic BI (1999) Mechanisms of action of and resistance to antitubulin agents: microtubule dynamics, drug transport, and cell death. J Clin Oncol 17:1061–1070
2. Tannock IF, de Wit R, Berry WR, Horti J, Pluzanska A, Chi KN, Oudard S, Theodore C, James ND, Turesson I et al (2004) Docetaxel plus prednisone or mitoxantrone plus prednisone for advanced prostate cancer. N Engl J Med 351:1502–1512
3. Malik B, Stillman M (2008) Chemotherapy-induced peripheral neuropathy. Curr Neurol Neurosci Rep 8:56–65
4. Hamel E (1992) Natural products which interact with tubulin in the vinca domain maytansine, rhizoxin, phomopsin A, dolastatins 10 and 15 and halichondrin B. Pharmacol Ther 55:31–51
5. Verrills NM, Kavallaris M (2005) Improving the targeting of tubulin-binding agents: lessons from drug resistance studies. Curr Pharm Des 11:1719–1733
6. Sanchez C, Mendoza P, Contreras HR, Vergara J, McCubrey JA, Huidobro C, Castellon EA (2009) Expression of multidrug resistance proteins in prostate cancer is related with cell sensitivity to chemotherapeutic drugs. Prostate 69:1448–1459
7. Leonard GD, Fojo T, Bates SE (2003) The role of ABC transporters in clinical practice. Oncologist 8:411–424
8. Chou TC, O'Connor OA, Tong WP, Guan Y, Zhang ZG, Stachel SJ, Lee C, Danishefsky SJ (2001) The synthesis, discovery, and development of a highly promising class of microtubule stabilization agents: curative effects of desoxyepothilones B and F against human tumor xenografts in nude mice. Proc Natl Acad Sci USA 98:8113–8118
9. Lin B, Catley L, LeBlanc R, Mitsiades C, Burger R, Tai YT, Podar K, Wartmann M, Chauhan D, Griffin JD, Anderson KC (2005) Patupilone (epothilone B) inhibits growth and survival of multiple myeloma cells in vitro and in vivo. Blood 105:350–357
10. Lee FY, Borzilleri R, Fairchild CR, Kim SH, Long BH, Reventos-Suarez C, Vite GD, Rose WC, Kramer RA (2001) BMS-247550 a novel epothilone analog with a mode of action similar to paclitaxel but possessing superior antitumor efficacy. Clin Cancer Res 7:1429–1437
11. Beckers T, Reissmann T, Schmidt M, Burger AM, Fiebig HH, Vanhoefer U, Pongratz H, Hufsky H, Hockemeyer J, Frieser M, Mahboobi S (2002) 2-aroylindoles, a novel class of potent, orally active small molecule tubulin inhibitors. Cancer Res 62:3113–3119
12. Chou TC, Zhang XG, Harris CR, Kuduk SD, Balog A, Savin KA, Bertino JR, Danishefsky SJ (1998) Desoxyepothilone B is curative against human tumor xenografts that are refractory to paclitaxel. Proc Natl Acad Sci USA 95:15798–15802
13. Giannakakou P, Sackett DL, Kang YK, Zhan Z, Buters JT, Fojo T, Poruchynsky MS (1997) Paclitaxel-resistant human ovarian cancer cells have mutant beta-tubulins that exhibit impaired paclitaxel-driven polymerization. J Biol Chem 272:17118–17125
14. Letourneau IJ, Slot AJ, Deeley RG, Cole SP (2007) Mutational analysis of a highly conserved proline residue in MRP1, MRP2, and MRP3 reveals a partially conserved function. Drug Metab Dispos 35:1372–1379
15. Tsuruo T, Iida-Saito H, Kawabata H, Oh-hara T, Hamada H, Utakoji T (1986) Characteristics of resistance to adriamycin in human myelogenous leukemia K562 resistant to adriamycin and in isolated clones. Jpn J Cancer Res 77:682–692

16. Fang L, Zhang G, Li C, Zheng X, Zhu L, Xiao JJ, Szakacs G, Nadas J, Chan KK, Wang PG, Sun D (2006) Discovery of a daunorubicin analogue that exhibits potent antitumor activity and overcomes P-gp-mediated drug resistance. J Med Chem 49:932–941
17. Chen C, Okayama H (1987) High-efficiency transformation of mammalian cells by plasmid DNA. Mol Cell Biol 7:2745–2752
18. Robey RW, Honjo Y, Morisaki K, Nadjem TA, Runge S, Risbood M, Poruchynsky MS, Bates SE (2003) Mutations at amino-acid 482 in the ABCG2 gene affect substrate and antagonist specificity. Br J Cancer 89:1971–1978
19. Bacher G, Nickel B, Emig P, Vanhoefer U, Seeber S, Shandra A, Klenner T, Beckers T (2001) D-24851, a novel synthetic microtubule inhibitor, exerts curative antitumoral activity in vivo, shows efficacy toward multidrug-resistant tumor cells, and lacks neurotoxicity. Cancer Res 61:392–399
20. Dethlefsen LA, Prewitt JM, Mendelsohn ML (1968) Analysis of tumor growth curves. J Natl Cancer Inst 40:389–405
21. Schinkel AH, Jonker JW (2003) Mammalian drug efflux transporters of the ATP binding cassette (ABC) family: an overview. Adv Drug Deliv Rev 55:3–29
22. Fares FA, Ge X, Yannai S, Rennert G (1998) Dietary indole derivatives induce apoptosis in human breast cancer cells. Adv Exp Med Biol 451:153–157
23. Ge X, Fares FA, Yannai S (1999) Induction of apoptosis in MCF-7 cells by indole-3-carbinol is independent of p53 and bax. Anticancer Res 19:3199–3203
24. Mahboobi S, Sellmer A, Eichhorn E, Beckers T, Fiebig HH, Kelter G (2005) Synthesis and cytotoxic activity of 2-acyl-1H-indole-4,7-diones on human cancer cell lines. Eur J Med Chem 40:85–92
25. Kuo CC, Hsieh HP, Pan WY, Chen CP, Liou JP, Lee SJ, Chang YL, Chen LT, Chen CT, Chang JY (2004) BPR0L075, a novel synthetic indole compound with antimitotic activity in human cancer cells, exerts effective antitumoral activity in vivo. Cancer Res 64:4621–4628
26. Liou JP, Wu CY, Hsieh HP, Chang CY, Chen CM, Kuo CC, Chang JY (2007) 4- and 5-aroylindoles as novel classes of potent antitubulin agents. J Med Chem 50:4548–4552
27. Liou JP, Wu ZY, Kuo CC, Chang CY, Lu PY, Chen CM, Hsieh HP, Chang JY (2008) Discovery of 4-amino and 4-hydroxy-1-aroylindoles as potent tubulin polymerization inhibitors. J Med Chem 51:4351–4355
28. Usui T, Kondoh M, Cui CB, Mayumi T, Osada H (1998) Tryprostatin A, a specific and novel inhibitor of microtubule assembly. Biochem J 333(Pt 3):543–548
29. Mahboobi S, Pongratz H, Hufsky H, Hockemeyer J, Frieser M, Lyssenko A, Paper DH, Burgermeister J, Bohmer FD, Fiebig HH et al (2001) Synthetic 2-aroylindole derivatives as a new class of potent tubulin-inhibitory, antimitotic agents. J Med Chem 44:4535–4553
30. Haldar S, Basu A, Croce CM (1997) Bcl2 is the guardian of microtubule integrity. Cancer Res 57:229–233
31. Kraus LA, Samuel SK, Schmid SM, Dykes DJ, Waud WR, Bissery MC (2003) The mechanism of action of docetaxel (Taxotere) in xenograft models is not limited to bcl-2 phosphorylation. Invest New Drugs 21:259–268
32. Morris PG, Fornier MN (2008) Microtubule active agents: beyond the taxane frontier. Clin Cancer Res 14:7167–7172
33. Peterson JK, Tucker C, Favours E, Cheshire PJ, Creech J, Billups CA, Smykla R, Lee FY, Houghton PJ (2005) In vivo evaluation of ixabepilone (BMS247550), a novel epothilone B derivative, against pediatric cancer models. Clin Cancer Res 11:6950–6958
34. Le HT, Schaldach CM, Firestone GL, Bjeldanes LF (2003) Plant-derived 3,3′-diindolylmethane is a strong androgen antagonist in human prostate cancer cells. J Biol Chem 278:21136–21145